

# INDUCTION OF HEMOLYSIS AND ERYPTOSIS BY OCCUPATIONAL POLLUTANT NICKEL CHLORIDE IS MEDIATED THROUGH CALCIUM INFLUX AND P38 MAP KINASE SIGNALING

MOHAMMAD A. ALFHILI<sup>1</sup>, HASSAN S. ALAMRI<sup>2</sup>, JAWAHER ALSUGHAYYIR<sup>1</sup>, and AHMED M. BASUDAN<sup>1</sup>

<sup>1</sup> King Saud University, Riyadh, Saudi Arabia

College of Applied Medical Sciences, Department of Clinical Laboratory Sciences

<sup>2</sup> King Saud bin Abdulaziz University for Health Sciences/King Abdullah International Medical Research Center, Riyadh, Saudi Arabia

College of Applied Medical Sciences, Department of Clinical Laboratory Sciences

## Abstract

**Objectives:** Nickel (Ni) is an abundant environmental hazard and an occupational pollutant. Exposure to Ni compounds is prevalent in electroplating workers and in the printing industry, among others. The toxicity of Ni manifests as dermatological, gastrointestinal, respiratory, allergic, and cardiovascular symptoms. In particular, hyperbilirubinemia and reticulocytosis have been detected in intoxicated subjects; an observation possibly implicating selective red blood cell (RBC) toxicity. Herein, the interaction of nickel chloride (NiCl<sub>2</sub>) with human RBCs and associated molecular mechanisms are described. **Material and Methods:** Cells from healthy donors were incubated for 24 h at 37°C in the presence or absence of 0.5–10 mM of NiCl<sub>2</sub>, and cytotoxicity was determined through hemoglobin leakage by colorimetry under different experimental conditions. Eryptotic markers were also identified by flow cytometry using Annexin-V-FITC tagging for phosphatidylserine (PS) exposure, light scatter properties for cellular dimensions, Fluo4/AM labeling for intracellular calcium, and H2DCFDA staining for reactive oxygen species (ROS). Additionally, small molecule inhibitors were used to probe the signaling pathways involved. **Results:** It was found that NiCl<sub>2</sub> at 10 mM caused profound intracellular calcium overload and significant calcium-dependent hemolysis. Also, NiCl<sub>2</sub> reduced forward scatter and increased side scatter, Annexin-positive cells, and ROS levels. Importantly, NiCl<sub>2</sub>-induced hemolysis was significantly attenuated by the exclusion of extracellular calcium, and in the presence of p38 MAP kinase (MAPK) inhibitor SB203580. **Conclusions:** It is concluded that NiCl<sub>2</sub> induces p38 MAPK-dependent hemolysis, and stimulates the canonical features of premature eryptosis. This report presents the first description of the molecular mechanisms underlying the hemolytic and eryptotic potential of NiCl<sub>2</sub> and, thus, may explain changes in hematological parameters observed in poisoning victims. *Int J Occup Med Environ Health.* 2022;35(1):1–11

## Key words:

calcium, p38 MAPK, oxidative stress, hemolysis, nickel, eryptosis

Funding: this study was supported by Deputyship for Research and Innovation, Ministry of Education in Saudi Arabia (project No. IFKSURG-1441-335 entitled “Research Group,” grant manager: Ministry of Education).

Received: December 15, 2020. Accepted: April 13, 2021.

Corresponding author: Mohammad A. Alfihli, King Saud University, College of Applied Medical Sciences, Department of Clinical Laboratory Sciences, Riyadh 12372, Saudi Arabia (e-mail: malfeehily@ksu.edu.sa).

## INTRODUCTION

Nickel (Ni), a transition metal found in the Earth's crust, is widely used in the manufacture of monetary coins, jewelry, batteries, stainless steel, and in electroplating [1,2]. Clinically relevant applications of Ni include alloys used in prosthetic devices in cardiovascular, dental, and orthopedic medicine [3]. Occupational exposure to Ni, as in mining and refinery, and in welding fumes, increases the risk of lung fibrosis and cancer [4,5]. Alarmingly, Ni was also found in abundance in ovarian tissue undergoing malignant transformation, and many other studies, both *in vitro* and *in vivo*, have provided evidence of its carcinogenicity [6]. Therefore, Ni compounds are classified as potential human carcinogens by the World Health Organization [2].

As an environmental pollutant, the ingestion of Ni in drinking water significantly increased reticulocytes and serum bilirubin levels [7], which may suggest a hemolytic onset. Although red blood cells (RBCs; erythrocytes) are devoid of intracellular organelles, they, nonetheless, execute 2 forms of programmed cell death – eryptosis [8] and necroptosis [9]. Eryptotic cells lose membrane asymmetry with phosphatidylserine (PS) exposure on the cell surface, along with elevated intracellular calcium, overproduction of reactive oxygen species (ROS), ceramide accumulation, and the activation of signaling enzymes including caspases, p38 MAP kinase (MAPK), protein kinase C (PKC), and casein kinase 1 $\alpha$  (CK1 $\alpha$ ). Necroptosis, on the other hand, is regulated by the necroptosome, consisting of receptor-interacting protein 1 (RIP1), RIP3, and mixed lineage kinase domain like pseudokinase (MLKL).

On the molecular level, Ni compounds have been shown to induce apoptosis in a number of cells including lung [2,5] and bronchial cells, and lymphocytes [6]. In addition, Ni exposure has been shown to elicit autophagy [2], oxidative stress, and genotoxicity in nucleated cells [6]. To date, little is known regarding the interaction of Ni with

human RBCs, and the present study was thus designed to examine if and how Ni influences RBC physiology and longevity.

## MATERIAL AND METHODS

### Chemicals and reagents

Pure NiCl<sub>2</sub> was purchased from MilliporeSigma (Burlington, MA, USA) and a stock solution of 0.5 M was prepared by dissolving 97.19 mg in 1.5 ml of phosphate-buffered saline (PBS; 137 mM NaCl, 2.7 mM KCl, 10 mM Na<sub>2</sub>HPO<sub>4</sub>, 1.8 mM KH<sub>2</sub>PO<sub>4</sub>, pH 7.4). Hank's Balanced Salt Solution (HBSS), Ca<sup>2+</sup>-free HBSS, Annexin-V-FITC, Fluo4/AM, 2',7'-dichlorodihydrofluorescein diacetate (H<sub>2</sub>DCFDA), pan-caspase inhibitor zVAD(OMe)-FMK (zVAD), p38 MAPK inhibitor SB203580 (SB), PKC inhibitor staurosporin (StSp), CK1 $\alpha$  inhibitor D4476, RIP1 inhibitor necrostatin-2 (Nec-2), RIP3 inhibitor HS-1731, and MLKL inhibitor necrosulfonamide (NSA) were all purchased from Solarbio Life Science (Beijing, China). All dyes and inhibitors were dissolved in dimethyl sulfoxide (DMSO) at 10 or 100 mM.

### Blood samples and RBC isolation

Lithium heparin blood samples were collected from 9 healthy donors who provided written informed consents according to the Institutional Review Board approval at King Saud University (Project No. E-20-4544) and the Declaration of Helsinki. Red blood cell suspensions in PBS (1:3 v/v) were prepared by centrifugation at 839  $\times$  g for 15 min at room temperature. Control (0.1% DMSO) and experimental cells treated with 0.5–10 mM NiCl<sub>2</sub> (equivalent to 0.64–1.29 mg/ml NiCl<sub>2</sub> and 0.01–0.265 mg/ml Ni) were incubated at 5% hematocrit (0.6 $\times$ 10<sup>6</sup> cells/ $\mu$ l) for 24 h at 37°C before the analysis [10].

### Hemolysis

Cells were centrifuged at 13 000  $\times$  g for 1 min at room temperature. Hemoglobin concentration in the resulting supernatant, measured by light absorbance at 405 nm on

VersaMax plate reader (Molecular Devices, San Jose, CA, USA), was used to quantify the percentage of hemolyzed cells relative to that of cells suspended in distilled water (100% hemolysis). Plate and medium blanks were subtracted from each reading and then the following equation was applied:

$$\text{Hemolysis (\%)} = \frac{\text{absorbance (control or test samples)}}{\text{absorbance (distilled water)}} \times 100 \quad (1)$$

Hemolysis was expressed as a fold change compared to baseline values of the vehicle control [11].

### Phosphatidylserine exposure

Annexin-V-FITC was diluted to 0.5% v/v in a staining buffer composed of PBS with added 5 mM of CaCl<sub>2</sub>, and an aliquot of control and experimental cells was stained for 10 min at room temperature. The analysis was carried out in 10 000 events on FACSCanto™ II (Betcon-Dickinson, Franklin Lakes, NJ, USA). The percentage of cells with enhanced Annexin-V binding was identified using a marker following the excitation of cells at 488 nm and the capture of emitted light at 520 nm [10].

### Intracellular calcium

The stain Fluo4/AM was diluted to 2 μM in a staining buffer composed of PBS with added 5 mM of CaCl<sub>2</sub>, and aliquoted cells were stained for 30 min at 37°C. Following repeated washing, Fluo4 fluorescence, forward scatter (FSC), and side scatter (SSC) were examined in 10 000 events at the same spectra as the Annexin-V assay, and fluorescence was expressed as arbitrary units (a.u.) [8].

### Oxidative stress

The dye H<sub>2</sub>DCFDA was diluted to 5 μM in a staining buffer composed of PBS with added 5 mM of CaCl<sub>2</sub>, and aliquoted cells were stained for 30 min at 37°C. Excess, unbound dye was then removed by washing, and DCF fluorescence

in a.u. was examined in 10 000 events at the same spectra used for the Annexin-V assay [8].

### Statistical analysis

Results are presented as M±SEM of 3 independent experiments (N = 3), each performed in duplicate using 2 donors. Graphs were analyzed by Cyflogic™ software (CyFlo Ltd., Finland). The analysis was carried out using GraphPad Prism 8.0 (GraphPad Software, Inc., La Jolla, CA, USA). Comparisons were made using 1-way ANOVA followed by Dunnett's *post-hoc* test to compare treatment groups to the control or Tukey's *post-hoc* test to compare all treatment groups against each other. A p-value of <0.05 was considered statistically significant.

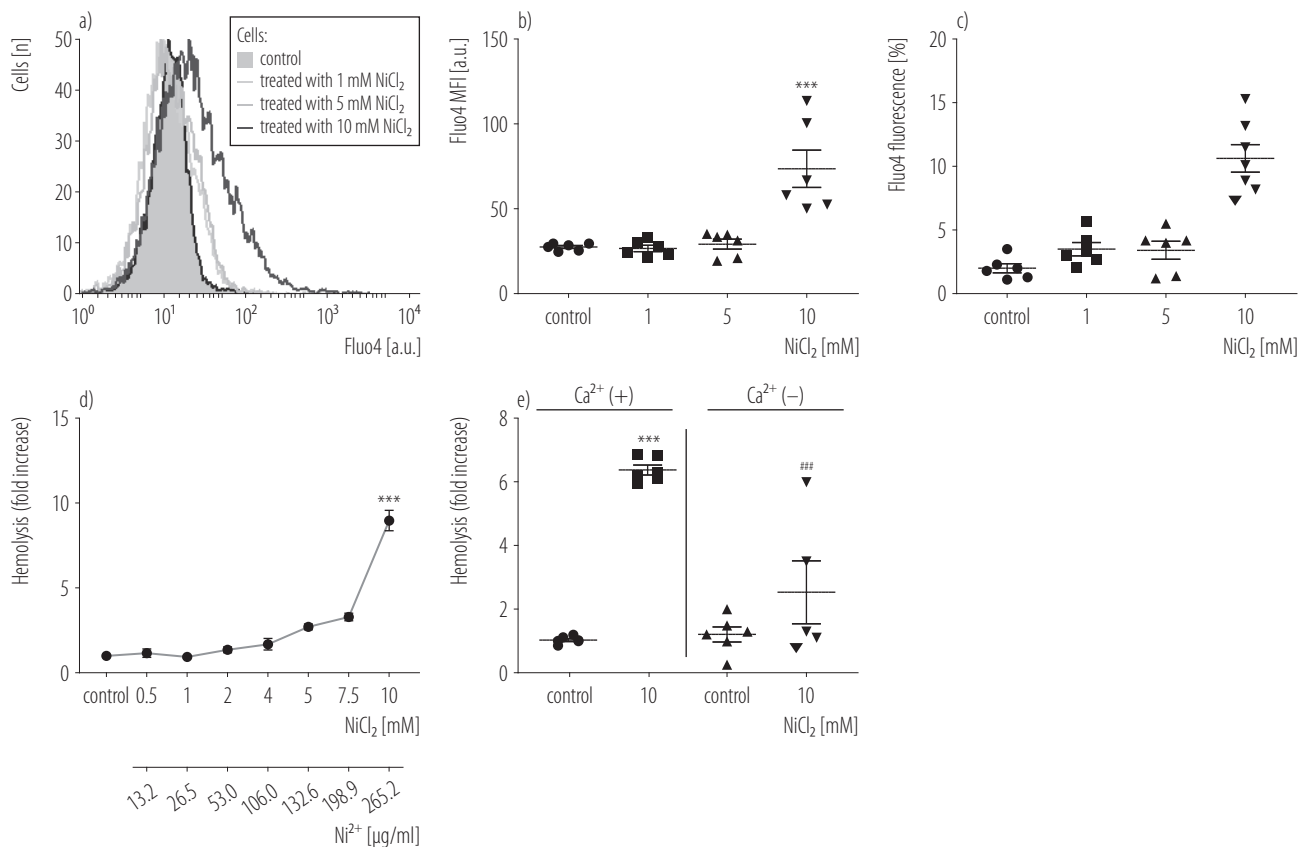
## RESULTS

### Cytosolic calcium concentration elevation in the presence of NiCl<sub>2</sub>

Calcium signaling plays a major role in triggering cell death [12]. To assess intracellular calcium levels, control and experimental cells were incubated in the presence or absence of 10 mM NiCl<sub>2</sub> for 24 h at 37°C, and were then loaded with 2 μM Fluo4/AM for 30 min at 37°C. Figure 1b shows that while 1 and 5 mM of NiCl<sub>2</sub> induced no significant increase in Fluo4 fluorescence (27.5±0.86 a.u. vs. 26.6±1.90 a.u. [p = 0.9990] and 29.2±2.91 a.u. [p = 0.9941], respectively), significantly enhanced fluorescence was observed in cells treated with 10 mM of NiCl<sub>2</sub> which showed 73.6±10.97 a.u. (p < 0.0001). Likewise, the percentage of cells with increased Fluo4 fluorescence, shown in Figure 1c, increased from 1.1±0.35% in the case of control cells to 3.5±0.52% (1 mM, p = 0.3994), 3.4±0.70% (5 mM, p = 0.4435), and 10.64±1.08% (10 mM, p < 0.0001). This indicates that NiCl<sub>2</sub> promotes cytosolic calcium accumulation.

### Induction of calcium-dependent hemolysis by NiCl<sub>2</sub>

Since increased calcium levels were observed, it was of interest to determine the hemolytic potential of NiCl<sub>2</sub>.



\*\*\*  $p < 0.001$  indicates a significant difference from control.

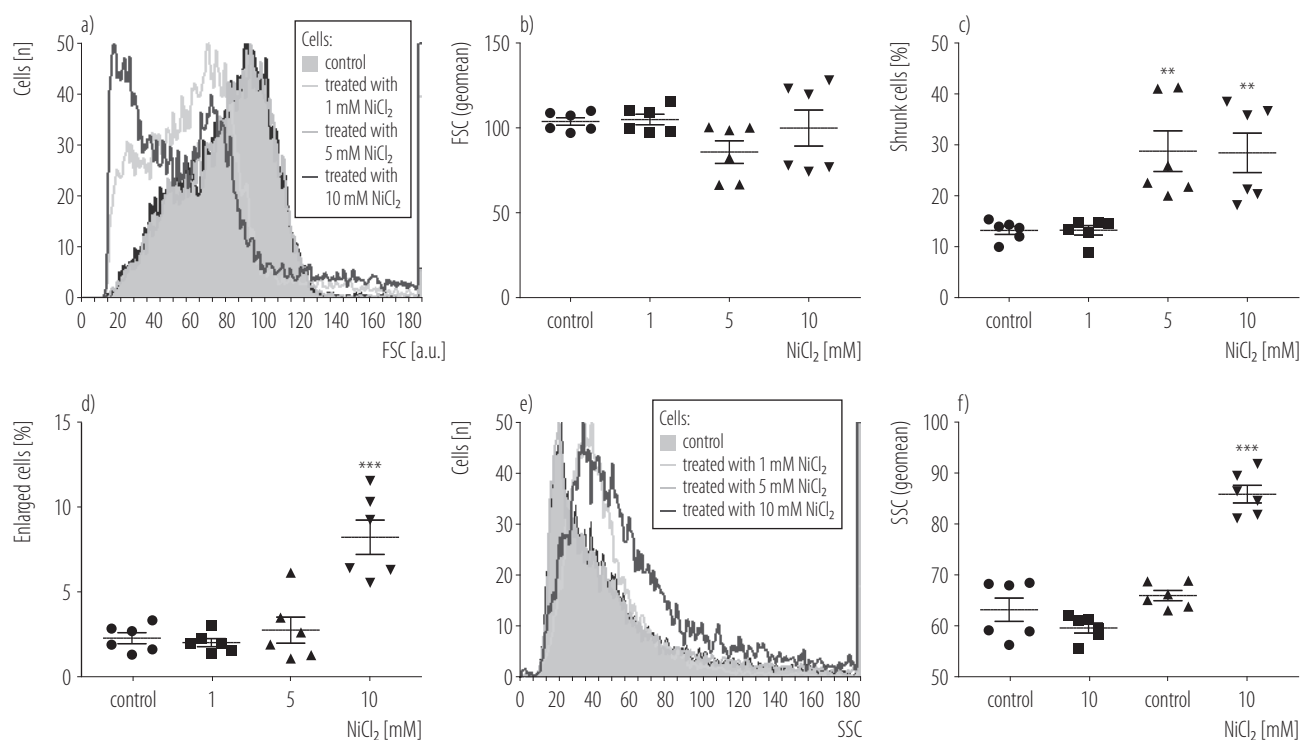
##  $p < 0.001$  indicates a significant difference from  $\text{NiCl}_2$ -treated cells in the presence of extracellular calcium. ANOVA followed by Dunnett's test was used for b), c), and d) while Tukey's was used for e).

Averages and SEM over independent experiments ( $N = 3$ ) are shown.

**Figure 1.** Nickel chloride ( $\text{NiCl}_2$ ) elevates cytosolic calcium and elicits calcium-dependent hemolysis: a) Fluo4 fluorescence histogram, b) mean fluorescence intensity (MFI) of Fluo4, c) cells with enhanced Fluo4 fluorescence, d) fold increase in hemolysis, e) fold increase in hemolysis with and without extracellular calcium in the presence or absence of 10 mM  $\text{NiCl}_2$

To this end, cells were incubated with 1–10 mM of  $\text{NiCl}_2$  for 24 h at 37°C and hemoglobin leakage was measured in the supernatant relative to that caused by distilled water. Hemolysis of tested conditions was normalized by the hemolysis level in the DMSO control and expressed as a fold change. As depicted in Figure 1d, the treatment of cells with increasing doses of  $\text{NiCl}_2$  elicited an increasing trend in hemolysis as appreciably observed at 5 mM ( $2.7 \pm 0.17$  folds,  $p = 0.9577$ ) and 7.5 mM ( $3.32 \pm 0.22$  folds,  $p = 0.7648$ ), and only attaining statistical significance at

10 mM ( $9.05 \pm 0.60$  folds,  $p < 0.0001$ ). Then, the contribution of extracellular calcium to  $\text{NiCl}_2$ -induced hemolysis was examined by treating the cells with 10 mM of  $\text{NiCl}_2$  in HBSS and in calcium-free HBSS. Figure 1e demonstrates a statistically significant decrease in hemolysis under the conditions of extracellular calcium elimination in cells treated with 10 mM of  $\text{NiCl}_2$  ( $6.45 \pm 0.2$  folds vs.  $2.47 \pm 1.02$  folds,  $p < 0.0001$ ). These data suggest that  $\text{NiCl}_2$  stimulates hemolysis secondary to cytosolic calcium accumulation from the extracellular space.



\*\*  $p < 0.01$  and \*\*\*  $p < 0.001$  indicate a significant difference from control (ANOVA, Dunnett's).

Averages and SEM over independent experiments ( $N = 3$ ) are shown.

**Figure 2.** Effect of nickel chloride ( $\text{NiCl}_2$ ) on cellular dimensions: a) forward scatter (FSC) histogram, b) geomean fluorescence values of FSC, c) control and experimental cells with reduced volume ( $<60$  a.u.), d) control and experimental cells with enlarged volume ( $>120$  a.u.), e) side scatter (SSC) histogram in control cells and cells treated with  $\text{NiCl}_2$ , f) geomean fluorescence of SSC values of control and experimental cells

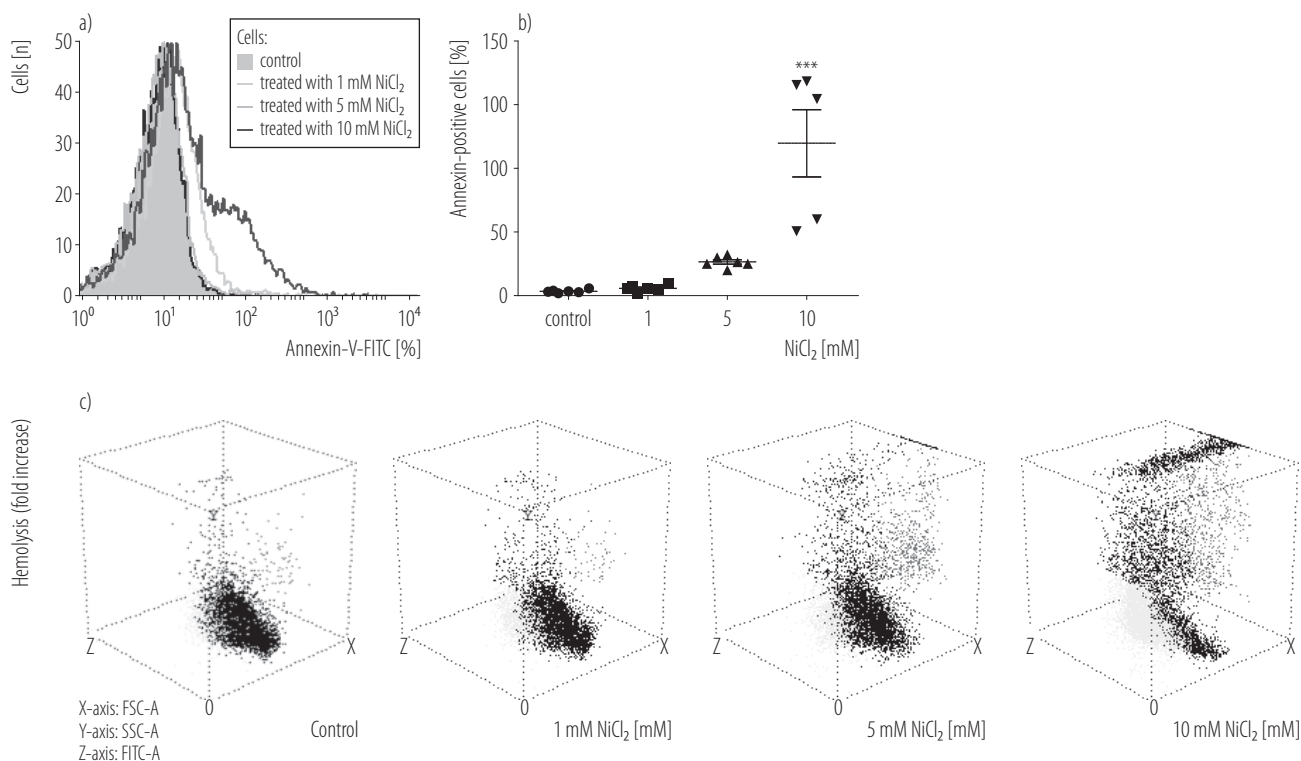
### Cell shrinkage and surface granularity caused by $\text{NiCl}_2$

A consequence of calcium entry is the activation of calcium-sensitive chloride channels and cell shrinkage [12]. To test the effect of  $\text{NiCl}_2$  on cellular morphology, FSC was used as a surrogate for cell size, while surface granularity was evaluated by SSC. While no significant alterations in the mean FSC were seen in control and treated cells (Figure 2b), the percentage of shrinking cells significantly increased from  $13.32 \pm 0.79\%$  in the case of control cells to  $28.82 \pm 4.0\%$  ( $p = 0.0026$ ) and  $28.48 \pm 3.85\%$  ( $p = 0.0032$ ) following treatment with 5 mM and 10 mM of  $\text{NiCl}_2$ , respectively (Figure 2c). Moreover, as depicted in Figure 2d, significantly increased numbers of enlarged cells were only observed at 10 mM of  $\text{NiCl}_2$  ( $2.28 \pm 0.32\%$  vs.  $8.23 \pm 1.01\%$ ,

$p < 0.0001$ ). Also, Figure 2f shows SSC values of  $63.19 \pm 2.30$  a.u. in control cells and a statistically significant increase in SSC values to  $85.91 \pm 1.72$  a.u. ( $p < 0.0001$ ) in cells treated with 10 mM of  $\text{NiCl}_2$ . Collectively, these observations indicate that  $\text{NiCl}_2$  induces cell shrinkage and enhanced cell surface complexity – 2 morphological characteristics typical of eryptotic cells.

### Phosphatidylserine exposure stimulated by $\text{NiCl}_2$

Cell membrane scrambling represents an early sign of eryptosis [8]. To investigate the pro-eryptotic activity of  $\text{NiCl}_2$ , cells were incubated with 1–10 mM of  $\text{NiCl}_2$  for 24 h at  $37^\circ\text{C}$  and were then labeled with Annexin-V-FITC for 10 min at room temperature in the dark. As seen in Figure 3b, although  $\text{NiCl}_2$  increased the percentage



\*\*\*  $p < 0.001$  indicates a significant difference from control (ANOVA, Dunnett's).

Averages and SEM over independent experiments ( $N = 3$ ) are shown.

**Figure 3.** Nickel chloride ( $\text{NiCl}_2$ ) stimulates phosphatidylserine (PS) exposure: a) Annexin-V-FITC fluorescence histogram in control and experimental cells treated with  $\text{NiCl}_2$ , b) Annexin-V-positive control and experimental cells, c) three-dimensional dot plots relating forward scatter (FSC) and side scatter (SSC) values to Annexin binding

of PS-exposing cells from  $1.51 \pm 0.2\%$  in the case of control to  $2.43 \pm 0.40\%$  (1 mM  $\text{NiCl}_2$ ,  $p = 0.9977$ ) and to  $10.75 \pm 0.68\%$  (5 mM  $\text{NiCl}_2$ ,  $p = 0.3509$ ), a statistically significant increase was only evident at 10 mM of  $\text{NiCl}_2$  ( $1.51 \pm 0.2\%$  vs.  $48.0 \pm 10.58\%$ ,  $p < 0.0001$ ). Thus, in addition to hemolysis,  $\text{NiCl}_2$  also leads to phospholipid scrambling and PS externalization to the outer membrane leaflet – a characteristic feature of eryptosis.

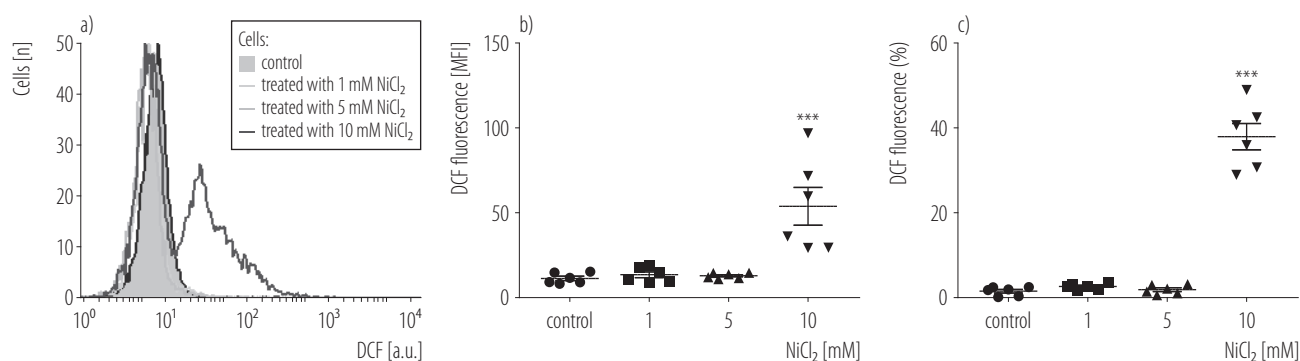
### Oxidative stress promoted by $\text{NiCl}_2$

Oxidative stress primes cells for eryptosis [10]. Intracellular ROS levels were, therefore, determined by DCF fluorescence following the incubation of cells for 24 h at  $37^\circ\text{C}$  with or without 1–10 mM of  $\text{NiCl}_2$ . As shown in Figure 4b, DCF in control cells ( $11.37 \pm 1.26$  a.u.) was significantly

enhanced following exposure to 10 mM of  $\text{NiCl}_2$  to  $53.82 \pm 11.13$  a.u. ( $p = 0.0001$ ). Similarly,  $\text{NiCl}_2$  increased the percentage of cells showing enhanced DCF fluorescence from  $1.60 \pm 0.72\%$  in control cells to  $38.03 \pm 3.65\%$  ( $p < 0.0001$ ) in 10 mM-treated cells. Altogether, oxidative stress seems to play a pivotal role in  $\text{NiCl}_2$ -induced cell death.

### Attenuation of $\text{NiCl}_2$ -induced hemolysis by SB203580

Signaling pathways play a central role in cell survival and death. To probe the involvement of signaling mediators in  $\text{NiCl}_2$  toxicity to RBCs, a small molecule inhibitor approach was employed as previously shown by these and other authors [11,13]. Cells exposed to 10 mM of  $\text{NiCl}_2$



\*\*\*  $p < 0.001$  indicates significant difference from control (ANOVA, Dunnett's).

Averages and SEM over independent experiments ( $N = 3$ ) are shown.

**Figure 4.** Nickel chloride ( $\text{NiCl}_2$ ) promotes oxidative stress: a) dichlorofluorescein (DCF) fluorescence histogram in control cells and cells treated with  $\text{NiCl}_2$ , b) mean fluorescence intensity (MFI) of DCF in control and experimental cells, c) control and experimental cells with enhanced DCF fluorescence

for 24 h at  $37^\circ\text{C}$  with or without  $10\ \mu\text{M}$  zVAD,  $2\ \mu\text{M}$  SB,  $0.5\ \mu\text{M}$  StSp, or  $5\ \mu\text{M}$  D4476 were analyzed for hemolysis as described earlier. Figure 5a shows that  $\text{NiCl}_2$ -induced cell death ( $1.0 \pm 0.007$  folds vs.  $11.49 \pm 0.48$  folds,  $p < 0.0001$ ) was not significantly reduced by zVAD ( $8.80 \pm 1.61$  folds,  $p = 0.0528$ ), StSp ( $10.83 \pm 0.62$  folds,  $p = 0.9535$ ), or D4476 ( $12.25 \pm 1.37$  folds,  $p = 0.9994$ ). However, significant reduction in hemolysis was observed in the presence of SB ( $4.20 \pm 0.16$ ,  $p < 0.0001$ ). These data seem to indicate that  $\text{NiCl}_2$ -induced hemolysis is mediated through p38 MAPK signaling.

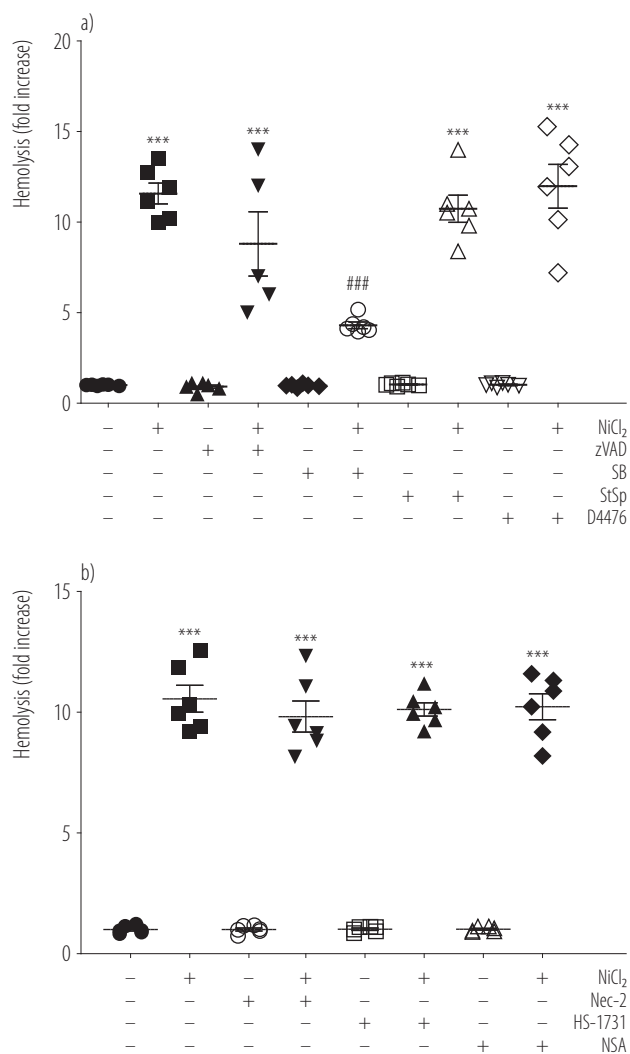
The participation of necroptosis mediators RIP1, RIP3, and MLKL was also examined. Figure 5b shows that no significant decrease in  $\text{NiCl}_2$ -induced hemolysis ( $10.51 \pm 0.48$  folds,  $p < 0.0001$ ) was observed in the presence of  $5\ \mu\text{M}$  Nec-2 ( $9.77 \pm 0.67$  folds,  $p = 0.5835$ ),  $100\ \text{nM}$  HS-1731 ( $10.03 \pm 0.22$  folds,  $p = 0.9303$ ) or  $5\ \text{nM}$  NSA ( $10.25 \pm 0.61$ ,  $p = 0.9850$ ). Accordingly,  $\text{NiCl}_2$  does not seem to stimulate necroptosis in human RBCs.

## DISCUSSION

Reports of Ni poisoning are underrepresented in literature and the current understanding of the molecular mechanisms governing Ni toxicity is severely deficient. This study reports a novel activity of  $\text{NiCl}_2$  which is the stim-

ulation of hemolysis and eryptosis in human RBCs. Although rarely reported, cases of accidental exposure to Ni compounds often range from mild and transient symptoms to severe and fatal outcomes. Poisoning victims are often exposed to Ni quantities ranging 73–3300 mg, and contaminated drinking water in 1 report had 2 mg/mL of Ni, with total ingestion of 3000 mg [7]. In the present study, Ni levels ranged 0.01–0.26 mg/mL, which are lower than exposure levels and within those shown to be toxic to nucleated cells [14,15]. It is noteworthy that the tested concentrations and associated toxic effects demonstrated in this study are expected to be encountered in cases of severe and fatal, acute poisoning or suicide attempts.

A significant increase in blood hemoglobin from 14.0 to 17.1 g/dl was noted in intoxicated individuals, along with reticulocytosis (up to  $217 \times 10^6$  cells/ml) and hyperbilirubinemia (up to  $43\ \mu\text{M}$ ). [7] These biochemical changes suggest enhanced erythropoiesis that may precede a hemolytic onset, which has previously been demonstrated in rodents [16]. Indeed, in this study, RBCs were found to be particularly susceptible to  $\text{NiCl}_2$  toxicity evident as dysregulated  $\text{Ca}^{2+}$  transport (Figures 1a–c) and overt hemolysis (Figures 1d–g), which may be ascribed to  $\text{Ca}^{2+}$ -induced membrane disruption and cytoskeletal instability [8,10]. In this regard, Ni resembles other metals



pathway in mouse epithelial skin cells through the Fas-caspase-8 axis [23], which is known to elicit PS exposure upon activation.

Beside intravascular hemolysis, eryptotic cells lose their flexibility and, consequently, tend to adhere to the inner walls of blood vessels, which increases the risk of thrombosis [24]. In cases of excessive eryptosis, the subsequent removal of RBCs from the bloodstream outweighs the rate of erythropoiesis in the bone marrow, which ultimately results in anemia. Of note, eryptosis is a common feature in a variety of pathological conditions including diabetes mellitus, hepatic and renal failure, and cancer [8].

Oxidative stress exacerbates hemolysis and eryptosis as the overproduction of ROS damages membrane proteins and lipids [10]. Along those lines, oxidatively damaged RBCs transport oxygen at a much lower rate than healthy cells, and the excess accumulation of ROS promotes cellular aging and inflammation [25]. This is in congruence with lipid peroxidation and diminished RBC antioxidants detected in workers exposed to Ni [26]. In fact, ROS production and RBC death are similarly exerted by the gold salt auranofin [8], as was demonstrated in Ni-treated kidney cells, lymphocytes [14,27], cervical cells, and bronchial and lung epithelial cells. In particular, glutathione depletion in lung cells and the activation of Nrf2 antioxidant regulator in monocytes have been reported [23].

The small molecule inhibitor studies seem to highlight the role of p38 MAPK in NiCl<sub>2</sub>-induced hemolysis (Figure 5a). The role of p38 in triclosan-induced RBC death has recently been demonstrated [11], and other compounds have been found to similarly activate the enzyme in RBCs. As a major cell survival and death mediator in erythrocytes, p38 is a stress-sensing enzyme that is mainly activated under conditions of physical and chemical challenge [8]. Interestingly, it has been demonstrated that mice lacking mitogen- and stress-activated kinase (MSK1/2), which acts downstream of p38,

display augmented susceptibility to hemolytic and eryptotic stimuli [8].

## CONCLUSIONS

In conclusion, the current study presents new evidence of Ni toxicity to human RBCs, and reveals the underlying cellular mechanisms. The results presented show that Ni causes Ca<sup>2+</sup>-dependent hemolysis, and eryptosis characterized by the loss of cell membrane asymmetry and normal cellular morphology, disrupted ionic regulation, and oxidative stress. Nickel poisoning remains a global public health concern with adverse effects on ecosystems and selective toxicity to humans at concentrations of <0.01 µg/ml [28]. Respiratory and allergic disease, cancer, and congenital malformations have been associated with Ni exposure [29,30], and dedicated efforts to delineate the molecular mechanisms of Ni toxicity are, therefore, urgently needed.

## REFERENCES

1. Guo H, Liu H, Jian Z, Cui H, Fang J, Zuo Z, et al. Nickel induces inflammatory activation via NF-kappaB, MAPKs, IRF3 and NLRP3 inflammasome signaling pathways in macrophages. *Aging (Albany NY)*, 2019;11(23):11659–72, <https://doi.org/10.18632/aging.102570>.
2. Kang YT, Hsu WC, Wu CH, Hsin IL, Wu PR, Yeh KT, et al. Metformin alleviates nickel-induced autophagy and apoptosis via inhibition of hexokinase-2, activating lipocalin-2, in human bronchial epithelial cells. *Oncotarget*. 2017;8(62):105536–52, <https://doi.org/10.18632/oncotarget.22317>.
3. Rae T. The toxicity of metals used in orthopaedic prostheses. An experimental study using cultured human synovial fibroblasts. *J Bone Joint Surg Br*. 1981;63-B(3):435–40, <https://doi.org/10.1302/0301-620x.63b3.7263760>.
4. Beveridge R, Pintos J, Parent ME, Asselin J, Siemiatycki J. Lung cancer risk associated with occupational exposure to nickel, chromium VI, and cadmium in two population-based case-control studies in Montreal. *Am J Ind Med*. 2010;53(5):476–85, <https://doi.org/10.1002/ajim.20801>.

5. Di Bucchianico S, Gliga AR, Åkerlund E, Skoglund S, Wallinder IO, Fadeel B, et al. Calcium-dependent cyto- and genotoxicity of nickel metal and nickel oxide nanoparticles in human lung cells. *Part Fibre Toxicol.* 2018;15(1):32, <https://doi.org/10.1186/s12989-018-0268-y>.
6. Cameron KS, Buchner V, Tchounwou PB. Exploring the molecular mechanisms of nickel-induced genotoxicity and carcinogenicity: a literature review. *Rev Environ Health.* 2011;26(2):81–92, <https://doi.org/10.1515/reveh.2011.012>.
7. Sunderman FW Jr, Dingle B, Hopfer SM, Swift T. Acute nickel toxicity in electroplating workers who accidentally ingested a solution of nickel sulfate and nickel chloride, *Am J Ind Med.* 1988;14(3):257–66, <https://doi.org/10.1002/ajim.4700140303>.
8. Pretorius E, du Plooy JN, Bester J. A Comprehensive Review on Eryptosis. *Cell Physiol Biochem.* 2016;39(5):1977–2000, <https://doi.org/10.1159/000447895>.
9. LaRocca TJ, Stivison EA, Hod EA, Spitalnik SL, Cowan PJ, Randis TM, et al. Human-specific bacterial pore-forming toxins induce programmed necrosis in erythrocytes. *mBio.* 2014;5(5):e01251–14, <https://doi.org/10.1128/mBio.01251-14>.
10. Alamri HS, Alsughayyir J, Akiel M, Al-Sheikh YA, Basudan AM, Dera A, et al. Stimulation of calcium influx and CK-1alpha by NF-kappaB antagonist [6]-Gingerol reprograms red blood cell longevity. *J Food Biochem.* 2020;e13545, <https://doi.org/10.1111/jfbc.13545>.
11. Alfihili MA, Weidner DA, Lee MH. Disruption of erythrocyte membrane asymmetry by triclosan is preceded by calcium dysregulation and p38 MAPK and RIP1 stimulation. *Chemosphere.* 2019;229:103–11, <https://doi.org/10.1016/j.chemosphere.2019.04.211>.
12. Föller M, Lang F. Ion Transport in Eryptosis, the Suicidal Death of Erythrocytes. *Front Cell Dev Biol.* 2020;8:597, <https://doi.org/10.3389/fcell.2020.00597>.
13. Jemaà M, Mischitelli M, Fezai M, Almasry M, Faggio C, Lang F. Stimulation of Suicidal Erythrocyte Death by the CDC25 Inhibitor NSC-95397. *Cell Physiol Biochem.* 2016;40(3–4):597–607, <https://doi.org/10.1159/000452573>.
14. Chen CY, Wang YF, Huang WR, Huang YT. Nickel induces oxidative stress and genotoxicity in human lymphocytes. *Toxicol Appl Pharmacol.* 2003;189(3):153–9, [https://doi.org/10.1016/s0041-008x\(03\)00086-3](https://doi.org/10.1016/s0041-008x(03)00086-3).
15. Chen CY, Wang YF, Lin YH, Yen SF. Nickel-induced oxidative stress and effect of antioxidants in human lymphocytes. *Arch Toxicol.* 2003;77(3):123–30, <https://doi.org/10.1007/s00204-002-0427-6>.
16. Hopfer SM, Sunderman FW Jr, Reid MC, Goldwasser E. Increased immunoreactive erythropoietin in serum and kidney extracts. *Res Commun Chem Pathol Pharmacol.* 1984;43(2):299–305.
17. Cartledge J, Minhas S, Eardley I. The role of nitric oxide in penile erection. *Expert Opin Pharmacother.* 2001;2(1):95–107, <https://doi.org/10.1517/14656566.2.1.95>.
18. Rifkind JM, Mohanty JG, Nagababu E. The pathophysiology of extracellular hemoglobin associated with enhanced oxidative reactions. *Front Physiol.* 2014;5:500, <https://doi.org/10.3389/fphys.2014.00500>.
19. Balla G, Jacob HS, Eaton JW, Belcher JD, Vercellotti GM. Hemin: a possible physiological mediator of low density lipoprotein oxidation and endothelial injury. *Arterioscler Thromb.* 1991;11(6):1700–11, <https://doi.org/10.1161/01.atv.11.6.1700>.
20. Wagener FA, Eggert A, Boerman OC, Oyen WJ, Verhofs-tad A, Abraham NG, et al. Heme is a potent inducer of inflammation in mice and is counteracted by heme oxygenase. *Blood.* 2001;98(6):1802–11, <https://doi.org/10.1182/blood.v98.6.1802>.
21. Wlodkowic D, Telford W, Skommer J, Darzynkiewicz Z. Apoptosis and beyond: cytometry in studies of programmed cell death. *Methods Cell Biol.* 2011;103:55–98, <https://doi.org/10.1016/B978-0-12-385493-3.00004-8>.
22. Wong P. A basis of echinocytosis and stomatocytosis in the disc-sphere transformations of the erythrocyte. *J Theor Biol.* 1999;196(3):343–61, <https://doi.org/10.1006/jtbi.1998.0845>.
23. Guo H, Chen L, Cui H, Peng X, Fang J, Zuo Z, et al. Research Advances on Pathways of Nickel-Induced Apoptosis. *Int J Mol Sci.* 2015;17(1), <https://doi.org/10.3390/ijms17010010>.

24. Pretorius E. Erythrocyte deformability and eryptosis during inflammation, and impaired blood rheology. *Clin Hemorheol Microcirc.* 2018;69(4):545–50. <https://doi.org/10.3233/CH-189205>.
25. Mohanty JG, Nagababu E, Rifkind JM. Red blood cell oxidative stress impairs oxygen delivery and induces red blood cell aging. *Front Physiol.* 2014;5:84, <https://doi.org/10.3389/fphys.2014.00084>.
26. Gupta AD, Patil AM, Ambekar JG, Das SN, Dhundasi SA, Das KK. L-ascorbic acid protects the antioxidant defense system in nickel-exposed albino rat lung tissue. *J Basic Clin Physiol Pharmacol.* 2006;17(2):87–100, <https://doi.org/10.1515/jbcpp.2006.17.2.87>.
27. Wang YF, Shyu HW, Chang YC, Tseng WC, Huang YL, Lin KH, et al. Nickel (II)-induced cytotoxicity and apoptosis in human proximal tubule cells through a ROS- and mitochondria-mediated pathway. *Toxicol Appl Pharmacol.* 2012;259(2):177–86, <https://doi.org/10.1016/j.taap.2011.12.022>.
28. Sall ML, Diaw AKD, Gningue-Sall D, Efremova Aaron S, Aaron JJ. Toxic heavy metals: impact on the environment and human health, and treatment with conducting organic polymers, a review. *Environ Sci Pollut Res Int.* 2020;27(24):29927–42, <https://doi.org/10.1007/s11356-020-09354-3>.
29. Denkhaus E, Salnikow K. Nickel essentiality, toxicity, and carcinogenicity. *Crit Rev Oncol Hematol.* 2002;42(1):35–56, [https://doi.org/10.1016/s1040-8428\(01\)00214-1](https://doi.org/10.1016/s1040-8428(01)00214-1).
30. Das KK, Reddy RC, Bagoji IB, Das S, Bagali S, Mullur L, et al. Primary concept of nickel toxicity – an overview. *J Basic Clin Physiol Pharmacol.* 2018;30(2):141–52, <https://doi.org/10.1515/jbcpp-2017-0171>.